Radiotherapy and Oncology 108 (2013) 484–488

Contents lists available at SciVerse ScienceDirect

Radiotherapy and Oncology

journal homepage: www.thegreenjournal.com

Epidermal growth factor receptor

^{111}In-cetuximab-F(ab')$_2$ SPECT imaging for quantification of accessible epidermal growth factor receptors (EGFR) in HNSCC xenografts

Laura K. van Dijk [a,b,*], Bianca A.W. Hoeben [a], Hanneke Stegeman [a], Johannes H.A.M. Kaanders [a], Gerben M. Franssen [b], Otto C. Boerman [b], Johan Bussink [a]

[a] Department of Radiation Oncology; and [b] Department of Nuclear Medicine, Radboud University Nijmegen Medical Center, The Netherlands

ARTICLE INFO

Article history:
Received 15 April 2013
Received in revised form 21 June 2013
Accepted 21 June 2013
Available online 7 August 2013

Keywords:
Head and neck cancer
EGFR imaging
Cetuximab
SPECT
Preclinical

ABSTRACT

Background and purpose: Immunohistochemical epidermal growth factor receptor (EGFR) expression does not correlate with treatment response in head and neck squamous cell carcinomas (HNSCC). Aim was to apply the tracer ^{111}In-cetuximab-F(ab')$_2$ for EGFR microSPECT imaging and to investigate if tracer uptake correlated with response to EGFR-inhibition by cetuximab in HNSCC xenografts. Usage of F(ab)$_2$ fragments allows for shorter interval between tracer injection and imaging.

Materials and methods: Mice with HNSCC xenografts, SCCNij202, 153, 185 and 167 were imaged with microSPECT using ^{111}In-cetuximab-F(ab')$_2$. Subsequently, tumors were analyzed by autoradiography and immunohistochemistry and tracer concentration was determined. Tumor uptake was correlated with previously assessed response to cetuximab treatment.

Results: MicroSPECT imaging showed preferential uptake in HNSCC xenografts. Tumor-to-liver ratios were 3.1 ± 0.2 (SCCNij202), 2.8 ± 0.4 (SCCNij153), 2.0 ± 0.8 (SCCNij185), 2.0 ± 0.4 (SCCNij167). Immunohistochemical EGFR fractions (fEGFR) differed significantly between xenografts; 0.77 ± 0.07 (SCCNij202), 0.66 ± 0.11 (SCCNij153), 0.57 ± 0.19 (SCCNij185), 0.16 ± 0.10 (SCCNij167) ($p < 0.001$). Tumor fEGFR correlated with ^{111}In-cetuximab-F(ab')$_2$ tumor uptake ($r = 0.6$, $p < 0.01$) and tracer autoradiography ($r = 0.7$, $p < 0.0001$). Tumor uptake of ^{111}In-cetuximab-F(ab')$_2$ was proportionally associated with cetuximab treatment response in three out of four xenograft models.

Conclusion: ^{111}In-cetuximab-F(ab')$_2$ showed good tumor-to-background contrast on microSPECT imaging, allowing noninvasive assessment of EGFR expression *in vivo*, and possibly evaluation of treatment response to EGFR-inhibition.

 Radiotherapy and Oncology 108 (2013) 484–488

The epidermal growth factor receptor (EGFR) is overexpressed in the majority of head and neck squamous cell carcinomas (HNSCC) and denotes a poor clinical outcome [1]. Elevated EGFR expression has been related to radiation resistance due to its influence on microenvironmental factors such as tumor oxygenation status, DNA repair processes and proliferation [2–5]. Supplementing radiotherapy with the EGFR-inhibitor cetuximab has resulted in improved locoregional control and overall survival, though it is effective in only a subset of the patients [6]. So far, no conclusive predictive marker for response to cetuximab has been identified in HNSCC [7–15].

Immunohistochemical determination of EGFR expression in tumor biopsies from patients does not correlate with treatment response [16,17], in part potentially due to tumor heterogeneity on a macro- and microscopic level. Also, tumor physiological factors such as vascular permeability, blood perfusion, interstitial fluid pressure and necrosis may explain the absence of this correlation [18,19]; a high expression of EGFR on immunohistochemistry does not denote accessibility of EGFR to inhibitors. Receptor imaging with tracers that are administered systemically allows noninvasive visualization of the entire tumor and renders the possibility of monitoring therapeutic effects. Previously, cetuximab has been labeled with ^{111}Indium (^{111}In) [20]. The use of radiolabeled cetuximab-F(ab)$_2$ fragments may allow earlier imaging due to faster clearance kinetics, resulting in a high tumor-to-background contrast at earlier time points. This study evaluated the potential of ^{111}In-cetuximab-F(ab')$_2$ to determine EGFR expression in tumors noninvasively. We analyzed the association between tumor tracer uptake and the treatment responses of the same HNSCC xenograft models we reported earlier [15].

Materials and methods

Tumor models

Six to eight week old athymic BALB/*c* nu/nu mice were xenografted subcutaneously (s.c.) in the right hind leg with the human

* Corresponding author. Address: Department of Radiation Oncology, Radboud University Nijmegen Medical Center, P.O. Box 9101, 6500 HB Nijmegen, The Netherlands.
E-mail address: l.vandijk@rther.umcn.nl (L.K. van Dijk).

0167-8140/$ - see front matter © 2013 Elsevier Ireland Ltd. All rights reserved.
http://dx.doi.org/10.1016/j.radonc.2013.06.034

HNSCC lines SCCNij202, 153, 185 or 167. Tumors with a mean volume of 191 ± 28 mm^3 were used in the experiments. Animals were housed in filter-topped cages in a specific-pathogen-free unit in accordance with institutional guidelines. The Animal Welfare Committee of the Radboud University Medical Center Nijmegen approved the animal experiments.

Tracer synthesis, experimental design and image acquisition

Cetuximab-F(ab')$_2$ was produced from the intact IgG monoclonal antibody cetuximab (≈150 kDa) by pepsin digestion. After labeling with ^{111}In labeling purity and efficiency were determined as described previously, with minor modifications [21].

For biodistribution studies, ten mice per tumor model were injected i.v. with 5 μg ^{111}In-cetuximab-F(ab')$_2$ (0.78 ± 0.33 MBq) of which five control mice received an EGFR blocking dose (1000 μg of cetuximab) 3 days prior to tracer injection. For imaging studies, six mice were injected with 5 μg ^{111}In-cetuximab-F(ab')$_2$ (21.4 ± 6.4 MBq). A control mouse excess of unlabeled cetuximab was used to determine non-EGFR mediated uptake of ^{111}In-cetuximab-F(ab')$_2$. Images were acquired 24 h p.i. using an ultra high-resolution animal SPECT/CT scanner (U-SPECT-II; MILabs, Utrecht, the Netherlands). Mice were scanned in prone position under general anesthesia (isoflurane/N_2O) using the 1.0-mm diameter multi-pinhole collimator tube. SPECT scans were acquired for 60 min, followed by CT scans.

Mice were euthanized 24 h after tracer injection and tissue samples of relevant tissues were harvested, weighed and radioactivity uptake was determined in a γ-counter. Activity concentrations were calculated and corrected for radioactive decay, and expressed as percentage of injected dose per gram tissue (%ID/g).

Scans were reconstructed with MILabs software, using an ordered-subset expectation maximization algorithm with a voxel size of 0.375 mm. Tumor-to-liver uptake ratios were determined by drawing regions of interest (ROIs) around the tumor and in the liver (Inveon Research Workplace software version 3.0, Siemens Preclinical Solutions); mean pixel values were established by thresholding at 40% of maximum pixel value within tumor ROIs.

Autoradiography

Intratumoral distribution of the radiolabeled antibody fragments was determined by autoradiography. Tumors from mice injected with ^{111}In-cetuximab-F(ab')$_2$ were dissected and immediately snap-frozen in liquid nitrogen. Autoradiography was performed as described previously [22]. Briefly, 5 μm sections were exposed to a Fujifilm BAS cassette 2025 overnight (Fuji Photo Film, Tokyo, Japan) and scanned using a Fuji BAS-1800 II bioimaging analyzer at a pixel size of 50 × 50 μm. Images were processed with Aida Image Analyzer software (Raytest, Staubenhardt, Germany).

Immunohistochemical staining and analysis

Following autoradiography, the same sections were fixed in acetone (4 °C for 10 min). For detection of EGFR expression, goat

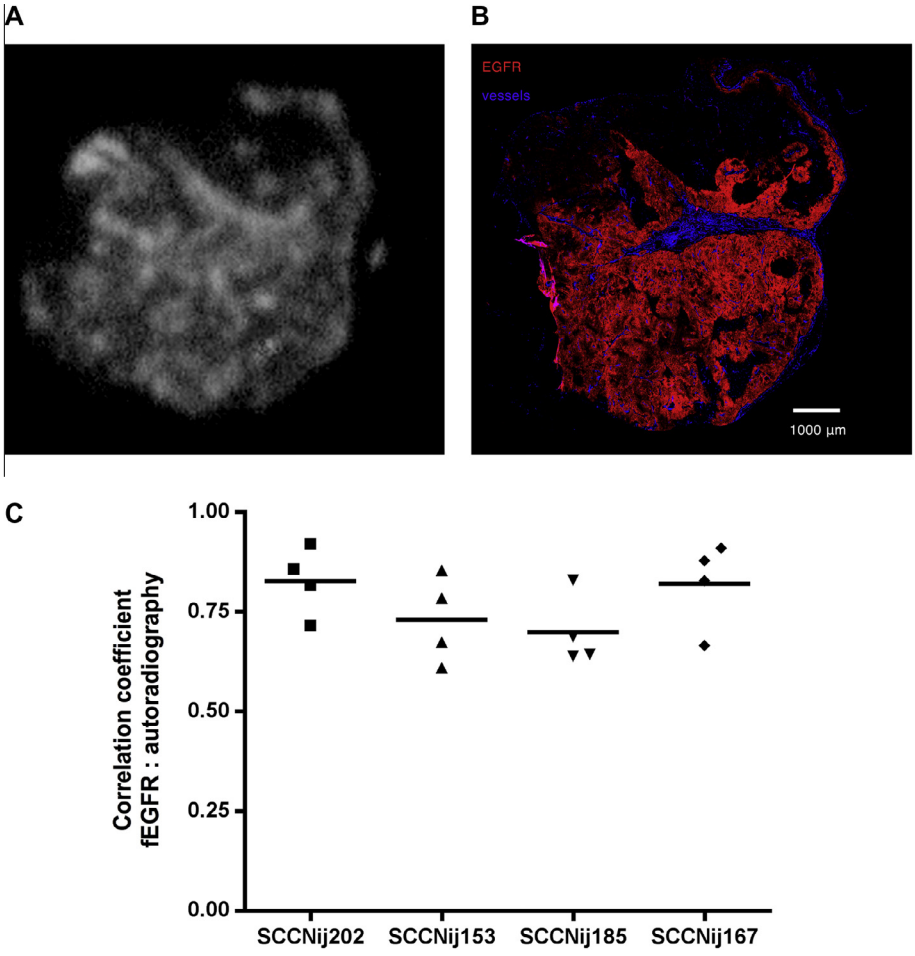

Fig. 1. ^{111}In-cetuximab-F(ab')$_2$ uptake measured by autoradiography (A), immunohistochemical staining of EGFR (red) and vessels (blue) (B) and the correlation coefficients between autoradiography and immunohistochemistry per xenograft model (n = 4 per group) (C).

anti-EGFR antibody (Santa Cruz Biotechnology Inc., Santa Cruz, CA, USA), followed by donkey anti-goat Cy3 (Jackson Immunoresearch, West Grove, PA, USA) was used. For visualization of the vasculature, undiluted rat anti-mouse endothelium 9F1 [20] was followed by incubation with chicken anti-rat-Alexa647 (Molecular Probes, Bleiswijk, The Netherlands).

Tumor sections were analyzed using a digital image analysis system, as described previously [23]. Briefly, tumor sections were scanned and grayscale images (pixel size, 2.59 × 2.59 μm) for vessels and EGFR were obtained and subsequently converted into binary images. Binary images were used to calculate the fraction of EGFR (fEGFR) relative to the total viable tumor area. Areas of necrosis were excluded from analysis.

Co-localization analysis

The autoradiography and immunohistochemistry gray-value images (grayscale range 0–255) were overlaid using Photoshop (CS4, version 11.0.2, San Jose, USA). The pixel and figure size of the immunohistochemistry images were bicubically rescaled to match those of the autoradiographic images for alignment (50 × 50 μm) and were successively upscaled (200 × 200 μm) to compensate for image co-registration errors and scattering of the tracer signal in the autoradiography images. After alignment, areas of necrosis in immunohistochemical analysis were masked in autoradiography images. Co-registered pixel gray-values and overlap coefficients were determined with ImageJ (version 1.43 m, JAVA-based image-processing package) using the JACoP plugin package.

Statistics

Statistical analyses were performed using Prism software version 4.0c (Graphpad, San Diego, USA). The Spearman, Pearson or ANOVA test was used to assess correlations between different parameters. Differences in uptake of the tracers were tested for significance using the nonparametric Mann–Whitney test. p-values $\leqslant 0.05$ were considered significant. Data are represented as mean ± standard deviation.

Results

The ^{111}In-cetuximab-F(ab')$_2$ tracer showed specific accumulation in EGFR expressing HNSCC xenografts: 5.7 ± 1.1%ID/g (SCCNij202), 7.5 ± 2.2%ID/g (SCCNij153), 2.7 ± 0.3%ID/g (SCCNij185), 2.2 ± 0.7%ID/g (SCCNij167) compared to mice receiving a blocking dose (1.7 ± 0.6%ID/g). Uptake in normal organs was similar for all four SCCNij models (Supplemental Table 1). Due to the rapid blood clearance a good tumor-to-blood contrast in all four HNSCC xenografts was achieved; SCCNij202: 14.1 ± 5.3; SCCNij153: 17.6 ± 5.6; SCCNij185: 6.2 ± 2.0; SCCNij167: 5.0 ± 1.7.

Immunohistochemical EGFR fractions differed significantly between the four xenograft models: SCCNij202: 0.77 ± 0.07; SCCNij153: 0.66 ± 0.11; SCCNij185: 0.57 ± 0.19; SCCNij167: 0.16 ± 0.10 ($p < 0.001$). For all tumors, autoradiography tracer location correlated statistically significantly with EGFR expression ($r = 0.68$, 95% confidence interval 0.68–0.70, $p < 0.0001$) (Fig. 1).

Tumor uptake of ^{111}In-cetuximab-F(ab')$_2$, quantified on microSPECT by tumor-to-liver-ratios correlated significantly with *ex vivo* activity uptake measurements ($r = 0.64$, $p < 0.01$) (Fig. 2A) and with fEGFR ($r = 0.61$, $p < 0.05$) (Fig. 2B). MicroSPECT images clearly showed preferential uptake in the tumor as evidenced by the tumor-to-liver ratios; 3.1 ± 0.2 (SCCNij202), 2.8 ± 0.4 (SCCNij153), 2.0 ± 0.8 (SCCNij185), 2.0 ± 0.4 (SCCNij167) (Fig. 3). In a previous study from our institution [15], SCCNij202 demonstrated the best growth-delay response to cetuximab. Here,

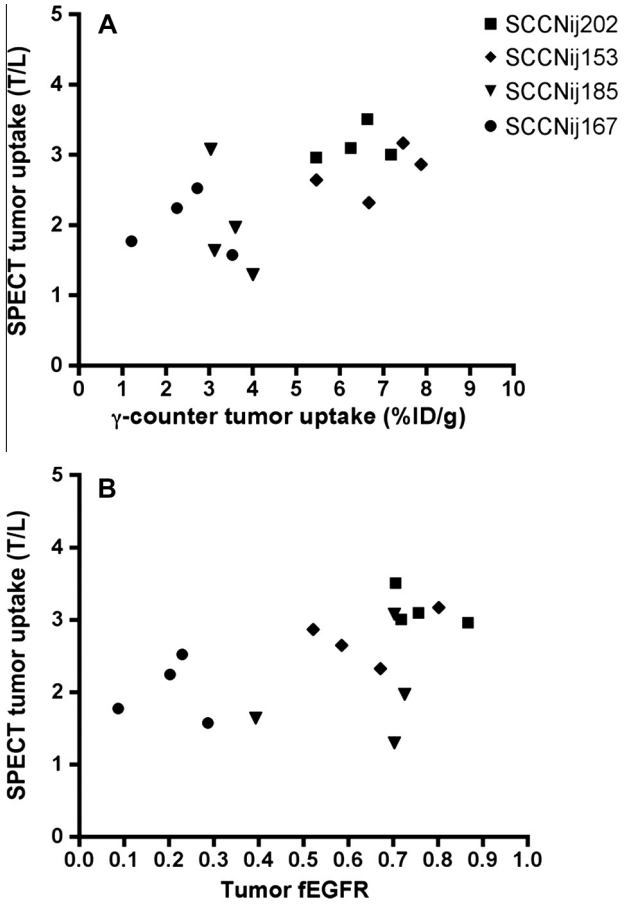

Fig. 2. Assessment of ^{111}In-cetuximab-F(ab')$_2$ microSPECT uptake correlated to *ex vivo* biodistribution studies ($r = 0.64$, $p < 0.01$) (A) and fraction EGFR staining in tumor sections (fEGFR) ($r = 0.61$, $p < 0.05$) (B) ($n = 16$). T/L = tumor-to-liver-ratio.

SCCNij202 showed the highest tumor uptake of ^{111}In-cetuximab-F(ab')$_2$, whereas the non-responder in the previous study (SCCNij167) displayed the lowest tracer uptake. SCCNij185 and SCCNij153 were moderate- to non-responders, while ^{111}In-cetuximab-F(ab')$_2$ uptake was low for SCCNij185 and high for SCCNij153.

Discussion

In this study, microSPECT images showed accumulation of ^{111}In-cetuximab-F(ab')$_2$ in all four HNSCC xenograft models and good tumor-to-background contrast as early as 24 h p.i. due to the rapid clearance from the background. EGFR fractions as determined immunohistochemically differed significantly between the four xenografts models and correlated with ^{111}In-cetuximab-F(ab')$_2$ uptake as measured by autoradiography and microSPECT scans. Previous preclinical studies have not shown a clear correlation between EGFR expression and cetuximab-tracer uptake when applying the whole IgG antibody [24–27]. One possible reason for this discrepancy could be that in the present study we used complete tumor sections for EGFR expression quantification and we used the same tumor sections for both autoradiographic and immunohistochemical analyses. In addition, we excluded necrosis and other non-tumor tissues from the tumor sections, eliminating potential bias from tracer localization in nonviable tissue. Furthermore, in a previous study we showed that when using F(ab')$_2$ fragments, optimal imaging could be performed already at 24 h p.i. in contrast to intact IgGs which need a significantly longer accretion time [20]. This could be important, as early imaging allows better

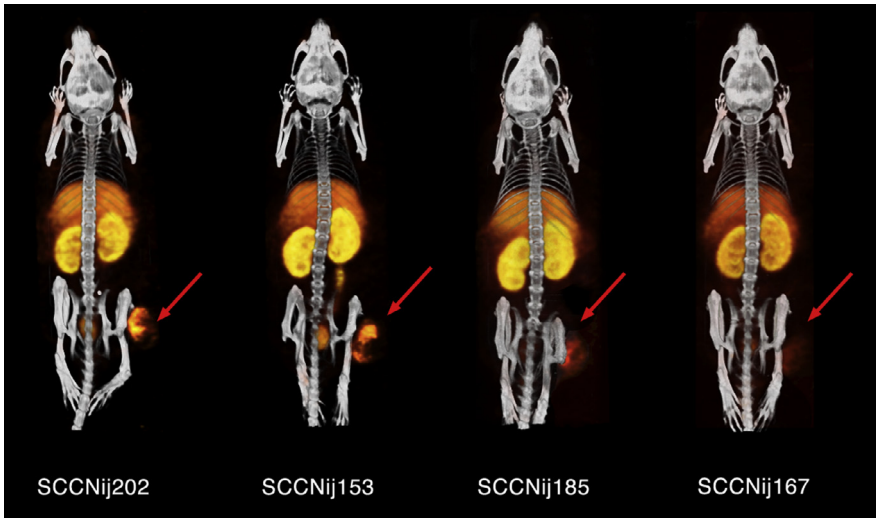

Fig. 3. MicroSPECT images of ^{111}In-cetuximab-F(ab')$_2$ obtained at 24 h p.i. of SCCNij202, 153, 185 and 167. Arrow = s.c. tumor location in right hind leg.

monitoring of tumor dynamics. It is also relevant for the often rapid cell turnover of hypoxic, but also non-hypoxic, cells and consequentially, their response to treatment [28].

In our previous study tumors with an intermediate immunohistochemical EGFR expression had a varying response to cetuximab [15]. In patients, it has been reported that EGFR expression as determined immunohistochemically is associated with survival but not with response to EGFR-inhibitors [29–31]. Even an inverse relationship between EGFR measured by immunohistochemistry and effectiveness of cetuximab was noted in a study where patients with low-to-moderate EGFR expression demonstrated an improved treatment response [32]. Similarly, in a preclinical study conducted by Gurtner et al., it has been shown that membrane and cytosolic EGFR expression do not correlate with local tumor control after radiotherapy or radiotherapy combined with cetuximab, possibly due to changes in EGFR expression induced after treatment [11]. Molecular imaging of EGFR-specific radiotracers has the advantage that only systemically accessible EGFR is measured and can be applied before and after treatment. In the current study, in three out of four HNSCC models, ^{111}In-cetuximab-F(ab')$_2$ tumor uptake was proportionally related to cetuximab response as high tumor uptake appeared to indicate a good cetuximab response and low uptake denoted a poor response. Only in one model with intermediate fEGFR and high tracer uptake, SCCNij153, the cetuximab response was discordant. This could be due to other dominant survival mechanisms in this particular tumor model that are not blocked by cetuximab, like dependency on the HER-pathway or alterations in the downstream signaling of the EGFR-mediated PI3-K/AKT pathway [15,33–35]. Important to note, as depicted in Fig. 2B, is that at similar levels of EGFR expression, a notable variation in tracer uptake can be seen. This is most apparent at fEGFR 0.7, where at least 7 tumors from three different models have a similar amount of EGFR expression but show dissimilar tracer uptake. Tumor uptake might be influenced by tumor microenvironmental factors, as well as by host factors. This emphasizes the aforementioned observations that EGFR-blockage added to radiotherapy may not result in the same effect on growth delay and local tumor control in individual tumors with a similar baseline EGFR expression. Hence, it accentuates the need for patient-specific approaches and for case-by-case analyses, where longitudinal non-invasive measurements are key and patients can serve as their own control.

In conclusion, this study shows the potential of ^{111}In-cetuximab-F(ab')$_2$ to rapidly determine EGFR expression in tumors noninvasively. Therefore, the ^{111}In-cetuximab-F(ab')$_2$ tracer can be a valuable asset for monitoring EGFR targeting in patients and for assessment of treatment response.

Conflict of interest

This study was financially supported by a research grant of the Dutch Cancer Society (2010-4688). The content is solely the responsibility of the authors and does not necessarily represent the official views of the funding organization.

Acknowledgements

We thank B. Lemmers-de Weem, K. Lemmens-Hermans, I. Lamers-Elemans, H. Arnts, H. Peters and J. Lok (Radboud University Medical Center Nijmegen) for their technical assistance.

Appendix A. Supplementary data

Supplementary data associated with this article can be found, in the online version, at http://dx.doi.org/10.1016/j.radonc.2013.06.034.

References

[1] Harari PM. Epidermal growth factor receptor inhibition strategies in oncology. Endocr Relat Cancer 2004;11:689–708.
[2] Bussink J, van der Kogel AJ, Kaanders JH. Activation of the PI3-K/AKT pathway and implications for radioresistance mechanisms in head and neck cancer. Lancet Oncol 2008;9:288–96.
[3] Bussink J, van der Kaanders JH, Kogel AJ. Microenvironmental transformations by VEGF- and EGF-receptor inhibition and potential implications for responsiveness to radiotherapy. Radiother Oncol 2007;82:10–7.
[4] Rademakers SE, Span PN, Kaanders JH, Sweep FC, van der Kogel AJ, Bussink J. Molecular aspects of tumour hypoxia. Mol Oncol 2008;2:41–53.
[5] Overgaard J. Hypoxic modification of radiotherapy in squamous cell carcinoma of the head and neck – a systematic review and meta-analysis. Radiother Oncol 2011;100:22–32.
[6] Bonner JA, Harari PM, Giralt J, et al. Radiotherapy plus cetuximab for squamous-cell carcinoma of the head and neck. N Engl J Med 2006;354:567–78.
[7] Argiris A, Lee SC, Feinstein T, et al. Serum biomarkers as potential predictors of antitumor activity of cetuximab-containing therapy for locally advanced head and neck cancer. Oral Oncol 2011;47:961–6.
[8] Licitra L, Mesia R, Rivera F, et al. Evaluation of EGFR gene copy number as a predictive biomarker for the efficacy of cetuximab in combination with chemotherapy in the first-line treatment of recurrent and/or metastatic squamous cell carcinoma of the head and neck: EXTREME study. Ann Oncol 2011;22:1078–87.

[9] Baumann M, Krause M. Targeting the epidermal growth factor receptor in radiotherapy: radiobiological mechanisms, preclinical and clinical results. Radiother Oncol 2004;72:257–66.
[10] Santiago A, Eicheler W, Bussink J, et al. Effect of cetuximab and fractionated irradiation on tumour micro-environment. Radiother Oncol 2010;97:322–9.
[11] Gurtner K, Deuse Y, Butof R, et al. Diverse effects of combined radiotherapy and EGFR inhibition with antibodies or TK inhibitors on local tumour control and correlation with EGFR gene expression. Radiother Oncol 2011;99:323–30.
[12] Stegeman H, Kaanders JH, Wheeler DL, et al. Activation of AKT by hypoxia: a potential target for hypoxic tumors of the head and neck. BMC Cancer 2012;12:463.
[13] Aerts HJ, Dubois L, Hackeng TM, et al. Development and evaluation of a cetuximab-based imaging probe to target EGFR and EGFRvIII. Radiother Oncol 2007;83:326–32.
[14] Wheeler DL, Dunn EF, Harari PM. Understanding resistance to EGFR inhibitors-impact on future treatment strategies. Nat Rev Clin Oncol 2010;7:493–507.
[15] Stegeman H, Kaanders JH, van der Kogel AJ, et al. Predictive value of hypoxia, proliferation and tyrosine kinase receptors for EGFR-inhibition and radiotherapy sensitivity in head and neck cancer models. Radiother Oncol 2013;106:383–9.
[16] Chung KY, Shia J, Kemeny NE, et al. Cetuximab shows activity in colorectal cancer patients with tumors that do not express the epidermal growth factor receptor by immunohistochemistry. J Clin Oncol 2005;23:1803–10.
[17] Mendelsohn J, Baselga J. Status of epidermal growth factor receptor antagonists in the biology and treatment of cancer. J Clin Oncol 2003;21:2787–99.
[18] Jain RK. Transport of molecules, particles, and cells in solid tumors. Annu Rev Biomed Eng 1999;1:241–63.
[19] Heldin CH, Rubin K, Pietras K, Ostman A. High interstitial fluid pressure – an obstacle in cancer therapy. Nat Rev Cancer 2004;4:806–13.
[20] Hoeben BA, Molkenboer-Kuenen JD, Oyen WJ, et al. Radiolabeled cetuximab: dose optimization for epidermal growth factor receptor imaging in a head-and-neck squamous cell carcinoma model. Int J Cancer 2011;129:870–8.
[21] Heskamp S, van Laarhoven HW, Molkenboer-Kuenen JD, et al. Optimization of IGF-1R SPECT/CT imaging using (111)In-labeled F(ab')(2) and Fab fragments of the monoclonal antibody R1507. Mol Pharm 2012.
[22] Hoeben BA, Kaanders JH, Franssen GM, et al. PET of hypoxia with 89Zr-labeled cG250-F(ab')2 in head and neck tumors. J Nucl Med 2010;51:1076–83.
[23] Rademakers SE, Rijken PF, Peeters WJ, et al. Parametric mapping of immunohistochemically stained tissue sections; a method to quantify the colocalization of tumor markers. Cell Oncol (Dordr) 2011;34:119–29.
[24] Ping Li W, Meyer LA, Capretto DA, Sherman CD, Anderson CJ. Receptor-binding, biodistribution, and metabolism studies of 64Cu-DOTA-cetuximab, a PET-imaging agent for epidermal growth-factor receptor-positive tumors. Cancer Biother Radiopharm 2008;23:158–71.
[25] Cai W, Chen K, He L, Cao Q, Koong A, Chen X. Quantitative PET of EGFR expression in xenograft-bearing mice using 64Cu-labeled cetuximab, a chimeric anti-EGFR monoclonal antibody. Eur J Nucl Med Mol Imaging 2007;34:850–8.
[26] Aerts HJ, Dubois L, Perk L, et al. Disparity between in vivo EGFR expression and 89Zr-labeled cetuximab uptake assessed with PET. J Nucl Med 2009;50:123–31.
[27] Niu G, Li Z, Xie J, Le QT, Chen X. PET of EGFR antibody distribution in head and neck squamous cell carcinoma models. J Nucl Med 2009;50:1116–23.
[28] Ljungkvist AS, Bussink J, Kaanders JH, et al. Hypoxic cell turnover in different solid tumor lines. Int J Radiat Oncol Biol Phys 2005;62:1157–68.
[29] Valentini AM, Pirrelli M, Caruso ML. EGFR-targeted therapy in colorectal cancer: does immunohistochemistry deserve a role in predicting the response to cetuximab? Curr Opin Mol Ther 2008;10:124–31.
[30] Labianca R, La Verde N, Garassino MC. Development and clinical indications of cetuximab. Int J Biol Markers 2007;22:S40–6.
[31] Dei Tos AP, Ellis I. Assessing epidermal growth factor receptor expression in tumours: what is the value of current test methods? Eur J Cancer 2005;41:1383–92.
[32] Burtness B, Goldwasser MA, Flood W, Mattar B, Forastiere AA. Phase III randomized trial of cisplatin plus placebo compared with cisplatin plus cetuximab in metastatic/recurrent head and neck cancer: an Eastern Cooperative Oncology Group study. J Clin Oncol 2005;23:8646–54.
[33] Shames DS, Carbon J, Walter K, et al. High heregulin expression is associated with activated HER3 and may define an actionable biomarker in patients with squamous cell carcinomas of the head and neck. PLoS One 2013;8:e56765.
[34] Nijkamp MM, Hoogsteen IJ, Span PN, et al. Spatial relationship of phosphorylated epidermal growth factor receptor and activated AKT in head and neck squamous cell carcinoma. Radiother Oncol 2011;101:165–70.
[35] Baumann M, Krause M, Dikomey E, et al. EGFR-targeted anti-cancer drugs in radiotherapy: preclinical evaluation of mechanisms. Radiother Oncol 2007;83:238–48.